

# Recovery of high temperature deformed Ni-Al alloys

T. V. NORDSTROM

*Sandia Laboratories, Albuquerque, New Mexico*

C. R. BARRETT

*Department of Materials Science and Engineering, Stanford University, Stanford, California, USA*

The flow-stress recovery of two high purity nickel aluminium alloys, containing zero and 5 vol%  $\gamma'$  (Ni<sub>3</sub>Al), deformed at 735°C has been studied for recovery times ranging from 0.1 to 100 h. Results show that the presence of a finely dispersed second phase does inhibit the recovery rate following high-temperature deformation. For short recovery times,  $t < 5$  h, neither alloy obeys the predictions of the diffusion-controlled dislocation network-growth recovery model. For longer times, the recovery of the solid solution alloy does agree with the model while that of the precipitation-hardened alloy continues to deviate.

The short-time recovery tests were used to obtain values for the recovery rate,  $r = d\sigma_i/dt$  and these values of  $r$  are used to predict values of the hardening rate,  $h = d\sigma_i/d\epsilon$ , from the relation  $\dot{\epsilon}_s = r/h$  where  $\dot{\epsilon}_s$  is the steady-state creep rate. The values of  $h$  obtained in this manner are in reasonable agreement with expected values, i.e.  $h \sim \mu/100$  where  $\mu$  is the shear modulus. Electron microscopy observations on as-deformed and recovered samples show good agreement between the measured changes in flow stress and the observed variations in dislocation density.

## 1. Introduction

Variation of the deformation temperature is known to influence the dislocation structure developed in a material and this structural variation should manifest itself through a variation in the kinetics of room-temperature flow-stress recovery. For example, prestraining at elevated temperatures under creep conditions produces a partially recovered substructure as recovery accompanies the deformation process. Subsequent comparison of the recovery behaviour of a creep substructure with that of a substructure produced by low-temperature deformation (no concurrent recovery during prestrain) should graphically reveal how the recovery process depends on dislocation arrangement. To date little quantitative work has been done to correlate recovery behaviour with changes in dislocation arrangement. This behaviour is of considerable interest, especially for high-temperature deformation where the kinetics of the recovery process are thought to control the

creep rate [1-7]. In addition, the short-time flow-stress recovery for high-temperature pre-strain tests provides a method of determining the recovery rate in the Bailey-Orowan [1-2] relation between work-hardening and recovery which is somewhat different from methods previously proposed. The Bailey-Orowan relation states simply that steady-state creep rate,  $\dot{\epsilon}_s$  can be described by the relation

$$\dot{\epsilon}_s = r/h \quad (1)$$

where  $r = (d\sigma_i/dt)_e$  is the dynamic recovery rate under applied stress  $\sigma$ ,  $h = (d\sigma_i/d\epsilon)_t$  is the hardening rate at the temperature of interest, and  $\sigma_i$  is the internal stress due to long range dislocation-dislocation interactions. Throughout the following discussion we assume that the above expressions for  $r$  and  $h$  represent quantities that can be measured experimentally. That is, we neglect the formal problems that any dislocation motion which occurs during recovery produces strain and that some dynamic recovery (cross-

slip, etc.) is included in measured values of  $h$ . These features are taken as second order effects. The working definition of  $r$  is then "recovery under zero macroscopic strain" and that of  $h$  is "work-hardening in the absence of climb-controlled recovery".

Previously proposed methods for evaluating  $r$  [8, 9] involve the measurement of transient effects during a creep test and the exact interpretation of the results is not completely clear because of the concurrent effects of both recovery and strain-hardening at elevated temperature. Also, most previous work has measured recovery and work-hardening rates in terms of applied stresses and not internal stresses. This can lead to errors in the determination of  $r$  and  $h$  [10].

The technique employed in this study to measure  $r$  was to strain a sample at elevated temperature and constant strain-rate into a region equivalent to steady-state creep where the sample deforms under constant applied stress. The internal stress is determined by cooling deformed samples under the applied stress, and then measuring the flow-stress at room-temperature. The difference in room-temperature flow-stress between an as-deformed sample and a fully annealed sample is then set equal to  $\sigma_i$ .  $\sigma_i$  therefore represents that portion of the flow-stress which can be equated with the driving force for recovery.

The recovery rate is determined by annealing samples under zero stress for various times following the prestrain and measuring the change in room-temperature flow-stress, i.e. change in  $\sigma_i$ . The rate of change of  $\sigma_i$  extrapolated to zero time is then a measure of the dynamic recovery rate for use in Equation 1. Using the imposed strain-rate and the measured recovery rate, the hardening rate can be calculated and compared with the hardening rate measured at room-temperature or hardening in the absence of climb. The primary assumptions involved in this method are that the principal portion of the driving force for recovery comes from the internal stress and not from the applied stress and that changes in  $\sigma_i$  directly reflect the recovery rate.

Although it is clear that an applied stress  $\sigma$  can aid the recovery process, a simple argument suggests that the effect is small. Consider recovery to be dislocation climb-controlled with the driving force for climb arising from line tension and the applied stress. To a first approximation the climb forces will be given by  $(\mu b^2)/L$  (line tension) and  $\sigma b$  (applied stress) where  $\mu$  is

the shear modulus,  $b$  is the Burgers vector and  $L$  the dislocation segment length. As the forces are additive, the thermal activation term in the climb rate (or recovery rate) expression is

$$\text{climb rate} \propto \exp\left(-\frac{Q}{kT}\right) \sinh\left\{\frac{\mu b^4}{LkT} + \frac{\sigma b^3}{kT}\right\} \quad (2)$$

where  $Q$  is the activation energy for climb and  $b^2$  is the activation area. Both  $(\mu b^4)/kTL$  and  $(\sigma b^3)/kT$  are much smaller than unity and Equation 2 can be approximated by

$$\text{climb rate} \propto \exp\left(-\frac{Q}{kT}\right) \left(\frac{\mu b^4}{LkT} + \frac{\sigma b^3}{kT}\right) \quad (3)$$

If  $\sigma \neq 0$  the climb rate is proportional to

$$\left(\frac{\mu b^4}{LkT} + \frac{\sigma b^3}{kT}\right) \sim 2 \frac{\mu b^4}{LkT}$$

where we have assumed creep conditions taking  $L$  to be the steady state dislocation spacing characteristic of the applied stress  $\sigma$  [ $(\sigma \sim \mu b)/L$ ]. Comparing this result with the case  $\sigma = 0$  where the rate is proportional to  $(\mu b^4/LkT)$ , the only difference is a factor of 2. There is no difference in stress or temperature dependence of the recovery rate. Thus the only error introduced by measuring recovery rates under zero applied stress is that they will be slightly lower than dynamic rates measured under creep conditions.

The correspondence between changes in  $\sigma_i$  and recovery is established by showing that  $\sigma_i \propto \sqrt{\rho}$  where  $\rho$  is the dislocation density. This relationship demonstrates that  $\sigma_i$  is a measure of the athermal component of the flow-stress due to dislocation-dislocation interactions. Independent measurements of  $\rho$  and  $\sigma_i$  throughout recovery establish the constancy of this relation and support the concept that changes in  $\sigma_i$  directly monitor changes in  $\rho$ .

For the present study, the Ni-Al system was selected for several reasons. Through variation in the Al content, the structure can be varied at testing temperature from a solid solution to a two-phase system with essentially the same matrix composition. The properties of the system are well known as far as structural stability [11] and strengthening due to the presence of a dispersion of  $\gamma'$ (Ni<sub>3</sub>Al) [12]. The system also has considerable technological importance since  $\gamma'$  has been shown to be a primary high-temperature strengthening mechanism in nickel-base superalloys [13].

TABLE I Detailed chemical composition of the two alloys studied

Alloy	At. %		Wt %					
	Al	Al	C	S	Co	Mn	Si	Cu
SS	11.9	5.85	0.003	< 0.001	< 0.01	< 0.01	0.013	0.012
LP	13.1	6.50	0.004	< 0.001	< 0.01	< 0.01	0.013	0.013

## 2. Experimental procedure

The two alloys used in this study were supplied through the courtesy of the International Nickel Company. The complete chemical analyses are given in Table I and the detailed preparation of the samples with a gauge section of  $2.5 \times 1.0 \times 0.005$  cm has been given previously [14]. From the equilibrium phase diagram, the 11.9% alloy (alloy SS) is a single-phase solid solution of Al in Ni and the 13.1% alloy (alloy LP) has about the same matrix composition with approximately 5 vol %  $\gamma'$  at the testing temperature of 735°C. Following solution-treating 0.5 h at 1050°C and precipitation-ageing 200 h at 735°C in dry nitrogen, the  $\gamma'$  is distributed as cubic particles approximately 1000Å in size and having a calculated interparticle spacing on the {111} planes of about 2500Å.

Fig. 1 is a schematic diagram of the testing procedure. The thermal treatments prior to straining are described in the preceding paragraph. Following the pre-ageing, the samples were heated under zero stress in a dual-elliptical quartz lamp furnace mounted on a servo-controlled hydraulic tensile machine operating under load control in a dry nitrogen atmosphere. Samples were held at 735°C for 0.5 h to stabilize the thermal gradients prior to testing. Temperature control along the gauge section was  $\pm 2^\circ\text{C}$ . Samples were deformed at constant elongation rate of  $0.01 \text{ min}^{-1}$  with measurement and control of length accomplished by a system of Inconel rods attached to the upper and lower grips, using a linear variable differential transformer to detect changes in distance between the two grips.

The samples were strained into a state equivalent to steady-state creep as shown in Fig. 1 where the applied stress is essentially constant with strain. The total strain introduced into the samples was 0.10 for alloy SS and 0.06 for alloy LP. The samples were then either rapidly cooled under load to preserve the creep substructure and prevent recovery from occurring, or else unloaded, recovered for some specific time at 735°C and then cooled to room-temperature. Cooling to 550°C, the temperature below which

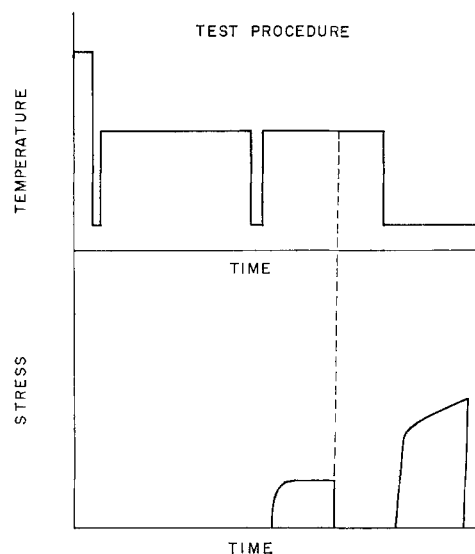


Figure 1 Schematic of ageing and testing procedure employed.

recovery was not observable for samples prestrained at room temperature, took approximately 1.5 min. For samples that underwent recovery anneals, treatments for 0.1 to 5 h were carried out in the tensile machine, while longer recovery treatments were done in a separate furnace.

Following deformation and recovery, a tensile test was run on the samples at room-temperature at the same strain-rate and the 0.2% offset yield strength measured. The results are evaluated in two ways. The first is the recovery parameter  $R$

$$R = \frac{\sigma_{u1} - \sigma_{y2}}{\sigma_{u1} - \sigma_{y1}}$$

where  $\sigma_{u1}$  is the yield strength for zero recovery time samples,  $\sigma_{y2}$  is the yield strength for samples recovered time  $t$  and  $\sigma_{y1}$  is the yield strength for a fully annealed sample. All yield strengths are defined as the stress to produce 0.2% strain. The recovery parameter varies from zero for no recovery to one for complete recovery. It is useful in comparing results from samples prestrained under different conditions

since it compares fractional changes in flow stress rather than absolute changes.

The second method of evaluating the results is in terms of that portion of the flow-stress which is the unrecovered work-hardening and due to dislocation-dislocation interactions. This quantity termed the internal stress  $\sigma_i$  is given by

$$\sigma_i = \sigma_{y2} - \sigma_{y1} \quad (5)$$

$\sigma_i$  and its variation with time is the quantity of interest when relating to high-temperature creep and recovery models.

Samples of the 0, 1.0, and 50 h recovery studies were examined using electron microscopy. Preparation of samples was the same as previously described [14] and the random-line intersection technique of dislocation density measurement [15] was used with at least forty different areas being counted on each sample.

### 3. Results and discussion

#### 3.1. Comparison with room-temperature results

Fig. 2 shows the time variation of the recovery parameter and internal stress for the two alloys prestrained at room-temperature and 735°C. On the recovery parameter basis, it can be seen that the basic difference between room- and high-temperature prestrain is the fraction of the recovery that occurs during the first 0.1 h. The slopes of the curves at the longer times for each alloy are approximately the same. The larger initial recovery in the room-temperature prestrain samples is probably due to short range effects such as dipole and loop annihilation and formation of interface dislocation networks as has been proposed previously [14]. Some portion of this type of recovery probably occurs during the prestraining at higher temperature but apparently does not accompany initial recovery of the 735°C prestrain substructure to the same large extent. The difference in the slope of the  $\sigma_i$  relations for the two prestrain temperatures is due to the larger amount of initial work-hardening,  $\sigma_{wh} = \sigma_{u1} - \sigma_{y1}$  for room-temperature prestrain. This essentially introduces a larger driving force,  $\sigma_i$ , for recovery. For the 735°C prestrain, the applied stress in the steady state region was  $1.3 \times 10^7$  dyn/cm<sup>2</sup> for alloy SS and  $2.27 \times 10^9$  dyn cm<sup>-2</sup> for alloy LP.

Fig. 3 shows a series of electron micrographs for alloy SS recovered for 0, 1.0 and 100 h for room-temperature prestrain and 0, 1.0 and 50 h for 735°C prestrain. The as-deformed state for

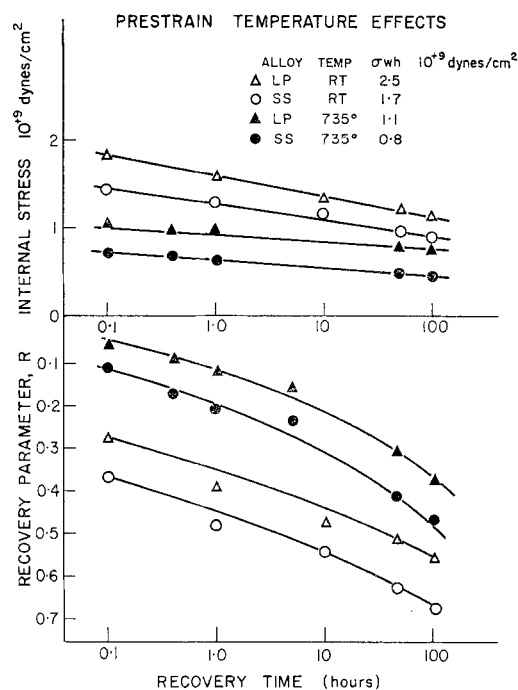


Figure 2 Effect of prestrain temperature on the variation of the internal stress and recovery parameter with time.

room-temperature is characterized by slip bands plus a fairly uniform overall distribution of dislocations. At 735°C the as-deformed state is a uniform three-dimensional distribution of dislocations with some evidence of two-dimensional networks developing as sub-boundaries, especially in regions adjacent to grain boundaries. This is quite similar to short-time recovery structures for room-temperature prestrain. Table II gives the measured dislocation densities for the samples shown in Fig. 3. Recovery for both temperatures of prestrain is characterized by an overall decrease in density of dislocations as recovery time increases. Aside from the as-deformed state, the structures for both temperatures are very similar.

For alloy LP, Fig. 4 shows an equivalent series of representative structures for 735°C prestrain with the interparticle dislocation density measurements given in Table II. The interface dislocations are not included in these reported values for  $\rho$ . The as-deformed structure is comparable to that seen for deformation at room temperature followed by recovery for a short time [14]. There are networks of dislocations at the  $\gamma'$ -matrix interface which act to relieve the lattice mismatch and a uniform distribution of interparticle

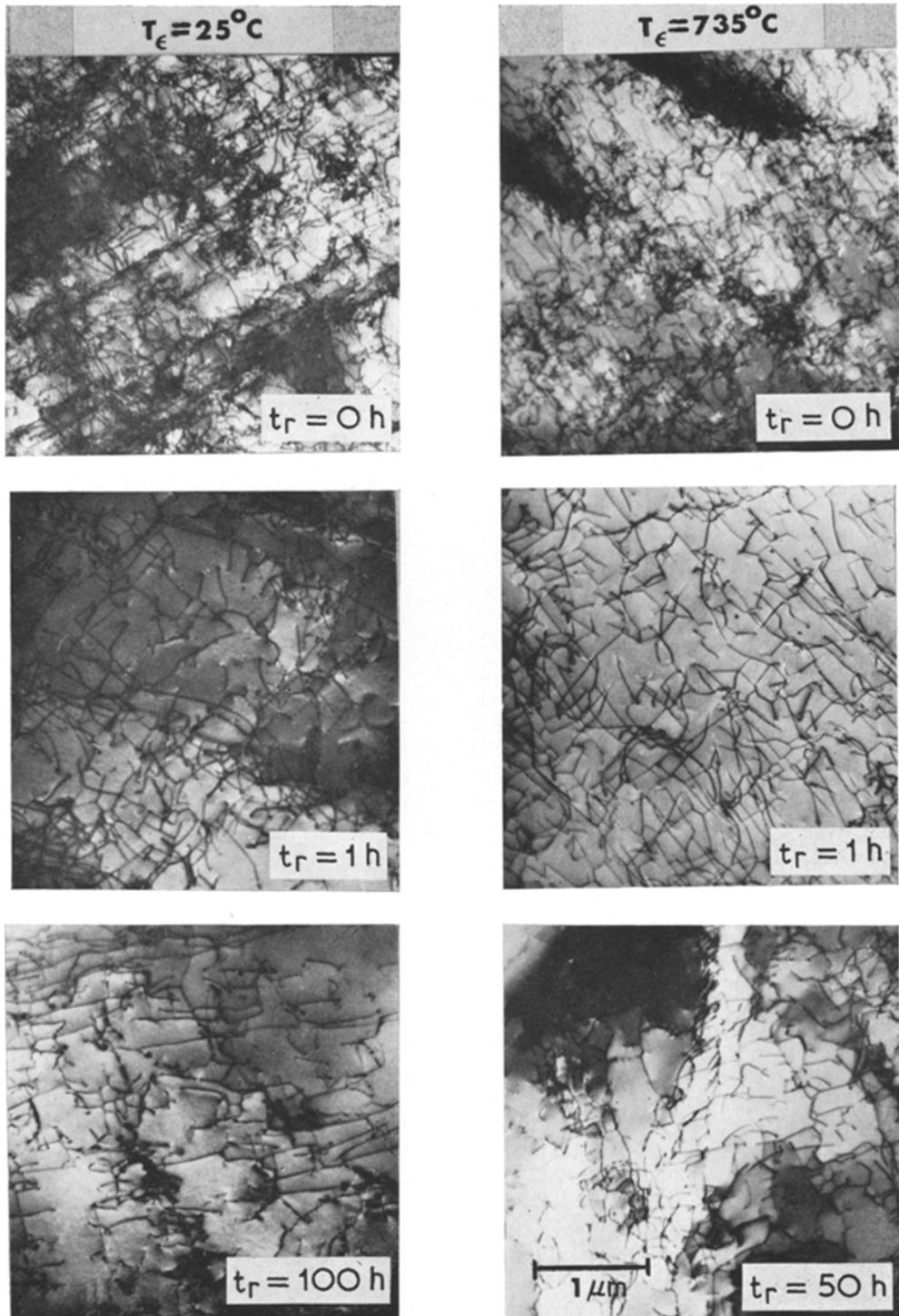


Figure 3 Comparison of deformed and recovered dislocation structures for alloy SS prestrained at 25 and 735°C.

TABLE II Dislocation density measurements from electron microscopy studies) (All values in  $10^9 \text{ cm}^{-2}$ )

Recovery time (h)	$\rho$ (Alloy SS) $RT$	Recovery time (h)	$\rho$ (Alloy SS) $735^\circ\text{C}$	$\rho$ (Alloy LP) $735^\circ\text{C}$
0	$12 \pm 1.7$	0	$7.4 \pm 2$	$13.9 \pm 2$
1	$7 \pm 1.7$	1	$6.9 \pm 2$	$12.2 \pm 2$
100	$5 \pm 1.7$	50	$5.4 \pm 2$	$9.9 \pm 2$

dislocations. Further recovery involves the reduction of measured dislocation density and distortion of the  $\gamma'$  particles by the interface dislocations. For this alloy also, the dislocation arrangements accompanying recovery are very similar for both low- and high-temperature prestrains except at very short recovery times. For recovery times of about 0.1 h, the low temperature prestrain samples show formation of  $\gamma'$ -matrix interfacial dislocation networks, a feature which is already present in the  $735^\circ\text{C}$  prestrained samples [14]. For both alloys, the dislocation density measurements agree with the relation  $\sigma_1 = \alpha \mu b \sqrt{\rho}$  with  $\alpha \approx 0.80$  where  $\mu$  is the shear modulus and  $b$  is the Burgers vector.

The assessment of the results in terms of the Friedel model [14, 16] for recovery by climb-controlled growth of a three-dimensional dislocation network\* is shown in Fig. 5. For the longer times,  $t > 5$  h, there is a good agreement for alloy SS with the prediction of the model that  $(1/\sigma_1)^2 \propto \text{time}$ . As would be expected from the model, the slope for the room-temperature and high-temperature prestrains is essentially the same. This agrees with the electron microscopy results, which show the recovery involves a decrease in the dislocation density with the dislocations distributed in a fairly uniform three-dimensional network of dislocations. For alloy LP, the longer time results show a considerably slower rate of recovery than that found for alloy SS. This is expected from the interaction of the dislocation network with the  $\gamma'$  particles. From the measured values of dislocation density, the average dislocation segment length in alloy LP in the as-strained condition is  $\sim 2000\text{\AA}$ . This can be compared with the average interparticle spacing of  $\sim 2500\text{\AA}$ . Thus a large portion of the dislocations must bow around adjacent particles and hence have a reduced driving force for recovery compared to that for alloy SS where the particles do not break up the continuity of the network or inhibit dislocation motion. It would

thus be expected that the precipitation hardened alloy would recover more slowly as is shown in Fig. 5 and predicted from creep results [17].

The disagreement with the model for short times in both alloys and at both temperatures indicates that all of the possible short range recovery processes (annihilation of loops, dipoles and the rearrangement of dislocation tangles) are not instantaneously eliminated at high-temperature but are an important portion of recovery during creep. Thus the use of the network growth model for recovery in formulating creep expressions [8] is subject to some doubt, at least for the relatively high strain-rates employed in the present study.

TABLE III Recovery and work-hardening rates as found from  $735^\circ\text{C}$  prestrain tests and room-temperature stress-strain curves

Alloy	$r$ $\text{dyn cm}^{-2} \text{ h}^{-1}$	$h_{\text{cal}}$ $\text{dyn cm}^{-2}$	$h_{\text{meas}}$ $\text{dyn cm}^{-2}$	$\sigma_i$ $\text{dyn cm}^{-2}$
SS	$1.8 \times 10^9$	$3 \times 10^9$	$8 \times 10^9$	$0.8 \times 10^9$
LP	$0.6 \times 10^9$	$1 \times 10^9$	$15 \times 10^9$	$1.1 \times 10^9$

### 3.2. Recovery – work-hardening rates

Fig. 6 shows the variation of  $\sigma_1$  with time for the short time recovery anneals of both alloys prestrained at  $735^\circ\text{C}$ . Approximating the slopes of the curves at zero time from the values of  $\sigma_1$  at times 0 and 0.1 h gives the recovery rates in Table III. These values are assumed to correspond to the dynamic recovery rate for high-temperature creep. The dynamic recovery rate in the solid solution is about three times that in the  $\gamma'$ -strengthened alloy despite the higher initial value of  $\sigma_1$  and thus higher driving force for recovery in alloy LP. This observation supports the view that the strong reductions in creep rate for materials with  $\gamma'$  present is due to the  $\gamma'$  inhibiting the recovery process as proposed in the previous section.

Also given in Table III are the values of the

\*This model predicts  $(1/\sigma_1)^2 = At + B$  where the parameter A contains the temperature dependence of the recovery process.

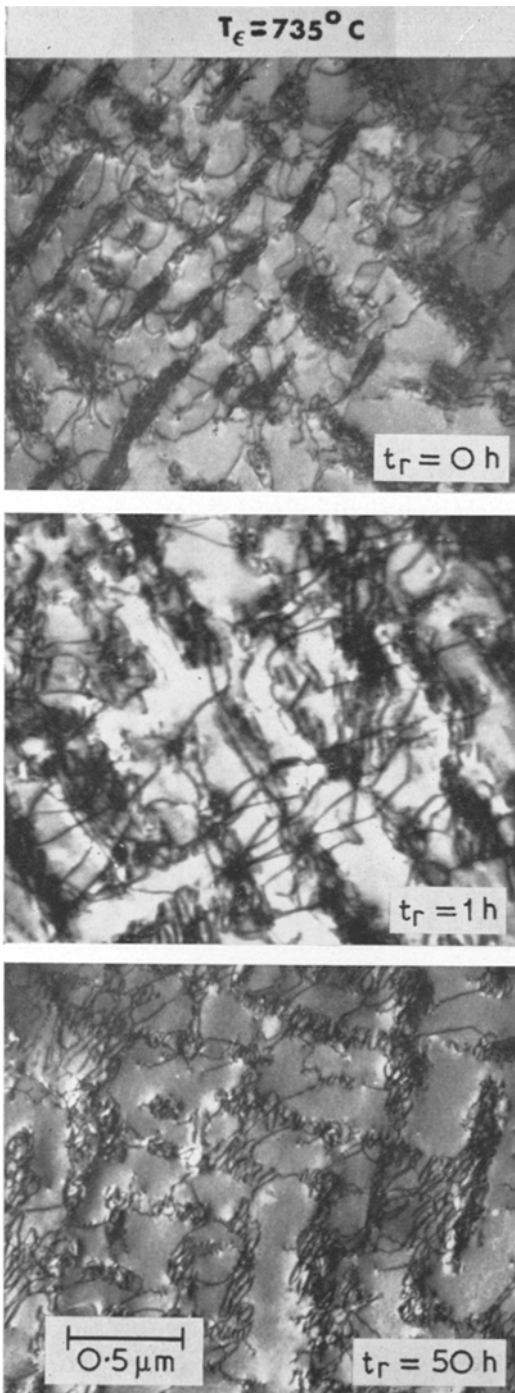


Figure 4 Deformed and recovered structures for alloy LP prestrained at 735°C.

hardening rate,  $h_{cal}$ , which were calculated using Equation 1, the measured recovery rate  $r$ , and the imposed strain rate  $\dot{\epsilon}_s = 0.6 \text{ h}^{-1}$ . The hardening

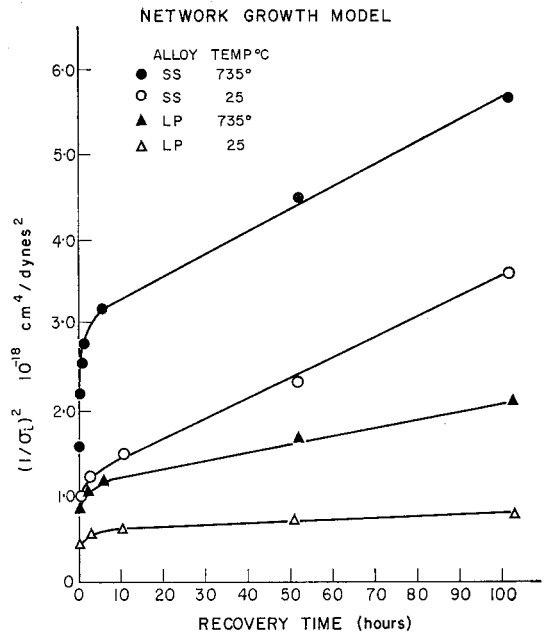


Figure 5 Comparison of room-temperature and 735°C prestrain tests with Friedel model for network growth recovery.

rate for alloy LP is less than that found for alloy SS despite the presence of the second phase which generally results in an increased work hardening rate. This effect can be explained if consideration is given to the variation in the internal stress level in the two alloys as listed also in Table III. The measured level of internal stress in alloy LP is considerably higher than that in alloy SS. This is due to the  $\gamma'$  in LP inhibiting the recovery process so that work-hardening builds up a higher level of internal stress before a balance of the two rates for steady-state creep is achieved. It has been shown experimentally [18] and for simple models [19] of work-hardening that the hardening rate varies inversely with the stress level to some power  $\sim 1$ . Thus the higher level of internal stress in LP results in a reduced work-hardening rate for this alloy and the data merely reflect the relationship  $h \propto 1/\sigma_1$ .

An attempt was also made to measure  $h$  from the slope of the room-temperature stress-strain curve, using the method suggested by Mitra and McLean [8], and compare these values with  $h_{cal}$ . Although there is some uncertainty as to which point on the  $\sigma - \epsilon$  curve the hardening rate should be taken, the present values were measured on a sample prestrained at high temperature and recovered, at the stress level

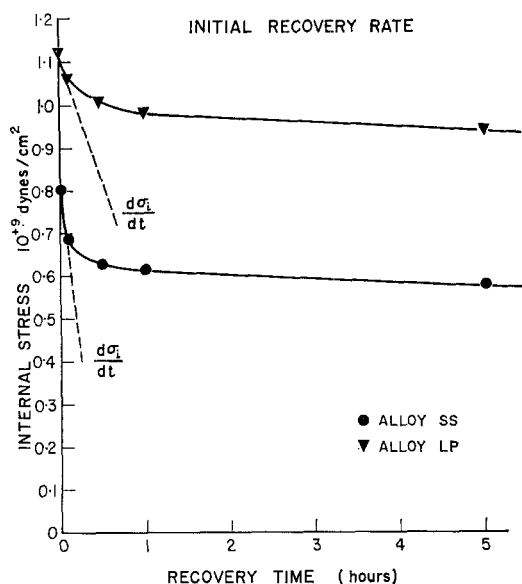


Figure 6 Determination of initial recovery rate for samples prestrained at 735°C.

where the internal stress is equal to the internal stress for zero recovery. This sample was chosen to approximate the substructure present during a creep test. The 100 h recovery test was used to obtain the values  $h_{meas}$ , given in Table III with correction being made for the temperature variation of the modulus [20]. As can be seen in Table III, these values of  $h_{meas}$  are about an order of magnitude higher than the values of  $h_{cal}$ . However, they do agree with values of  $h$  found using the same technique on other metals [8] and also with values of  $h$  found using incremental stress increases at elevated temperature and measuring the instantaneous strain [21].

There are two reasons to doubt the  $h_{meas}$  values. First the magnitude of these measured hardening rates ( $\sim \mu/10$ ) is considerably above the value expected from low-temperature strain-hardening ( $\sim \mu/200$ ). Previously reported values of  $h_{meas}$  as high as those observed here have been justified on the basis of their correlation with measured values of  $\dot{\epsilon}$  and  $r$ . However, it is likely that compensating errors existed in these earlier measurements of  $r$  and  $h$  [10]. In addition, the direct comparison of work-hardening rates for room- and high-temperature deformation is somewhat uncertain due to the considerable difference in the work-hardened structure for room- and elevated-temperature prestrain as Fig. 3 shows for alloy SS. On this basis it ap-

pears that the present technique for measuring  $r$  in terms of internal stress gives a more reasonable value for the hardening rate at elevated temperature than previous techniques that consider the applied stress only.

#### 4. Conclusions

The findings of this study can be summarized as follows:

1. The effect of increasing prestrain temperature on short-time recovery is to reduce the initial fractional recovery. This is due to the partial recovery of short range effects (annihilation of dipoles, loops and rearrangement of tangles) during the prestraining at elevated temperature.

2. For long-recovery times, the recovery rates are essentially independent of prestrain temperature and depend only on the magnitude of the internal stress with the results on the solid solution alloy showing good agreement with the Friedel model of network growth.

3. The short-time flow-stress recovery tests for high-temperature prestraining provide a new method for determining the recovery rate in the Bailey-Orowan relation in terms of internal stress. The technique predicts values of the high-temperature work-hardening rate that disagree with those found by previous investigators, but agree with the hardening rate values predicted by simple models of strain hardening and room-temperature strain-hardening tests.

4. The short-time recovery tests suggest that the Friedel model of network growth does not completely describe the recovery kinetics for either alloy during creep.

#### Acknowledgements

This project was supported partially by the Advanced Research Projects Agency through the Center for Materials Research at Stanford University and partially by the Atomic Energy Commission through contract number AT (04-3) 326-PA-17. Appreciation is expressed to the International Nickel Company for supplying the materials used in this investigation.

#### References

1. R. W. BAILEY, *J. Inst. Metals* **35** (1926) 26.
2. E. OROWAN, *J. West Scot. Iron & Steel Inst.* **54** (1946-47) 45.
3. A. H. COTTRELL and V. AYTEKIN, *J. Inst. Metals* **77** (1950) 389.
4. N. F. MOTT, *Phil. Mag.* **44** (1953) 742.
5. J. WEERTMAN, *J. Appl. Phys.* **28** (1957) 1185.



6. D. MCLEAN and K. F. HALE, Symposium on Structural Process in Creep, 1961 (London: Iron and Steel Inst. and Inst. of Metals) p. 19.
7. J. C. LI, *Acta Metallurgica* **11** (1953) 1269.
8. S. K. MITRA and D. MCLEAN, *Proc. Roy. Soc. [A]* **295** (1966) 288.
9. T. WATANABE and S. KARASHIMA, Proc. Intl. Conf. on Strength of Metals and Alloys, Tokyo (1967).
10. C. R. BARRETT, C. N. AHLQUIST, and W. D. NIX, *Metal Sci. J.* **4** (1970) 41.
11. A. J. ARDELL and R. B. NICHOLSON, *J. Phys. Chem. Solids* **27** (1966) 1793.
12. R. F. DECKER and J. R. MIHALISIN, *Trans. ASM* **62** (1969) 481.
13. A. TAYLOR and R. W. FLOYD, *J. Inst. Metals* **81** (1952-53) 451.
14. T. V. NORDSTROM and C. R. BARRETT, *J. Mater. Sci.* **7** (1972).
15. C. S. SMITH and L. GUTTMAN, *Trans. AIME* **197** (1953) 81.
16. J. FRIEDEL, "Dislocations" (Pergamon Press, Oxford, 1964) Ch. 8.
17. R. LAGNEBORG, *Metal Sci. J.* **3** (1969) 18.
18. J. R. LOW, "Properties of Metals in Materials Engineering" (Metals Park, Ohio, ASM, 1949).
19. G. I. TAYLOR, *Proc. Roy. Soc. A* **143** (1934) 307.
20. W. KOSTER, *Z. Metallk.* **39** (1948) 145.
21. Y. ISHIDA and D. MCLEAN, *J. Iron & Steel Inst.* **205** (1967) 88.

Received 3 January and accepted 26 January 1972.